TÜBİTAK

Review Article

Turk J Med Sci
2012; 42 (Sup.2): 1355-1364

E-mail: medsci@tubitak.gov.tr
doi:10.3906/sag-1111-9

Urothelial cancers: clinical and imaging evaluation

Halil ARSLAN, Fatih Mehmet TEZCAN, Oktay ALĞIN

Abstract: Urothelial cancers are currently diagnosed more commonly parallel to the recent developments in imaging techniques. Early diagnosis of these tumors, together with better treatment options, decreases the morbidity and the mortality significantly. This review aims to summarize the imaging findings of urothelial tumors, both at the pretreatment and posttreatment follow-up stage.

Key words: MRI, urography, hematuria, ureter cancer, urinary tract cancer, computed tomography, diagnosis, staging, ultrasound, urinary tract imaging, urothelial tumors

Introduction

Urothelial tumors originate from kidney collecting systems, ureters, the bladder, and the urethra. Their diagnosis and treatment approaches are quite different from those of parenchymal tumors of the kidney (1–3). Radiologists are expected to depict the presence, location, depth penetration, and local and distant metastatic status of these lesions, which usually present with painless hematuria (1–3). Herein, we aimed to review the radiologic approach, diagnostic methods, and differential diagnosis of urothelial tumors.

Urothelial tumors include pelvic, ureteral, bladder, and urethra tumors, and the majority of them are bladder tumors (3). They are most commonly seen in the 6th and 7th decades of life with a 4:1 male-to-female ratio (1–3). Transitional cell carcinoma (TCC) constitutes 95% of malignant urothelial tumors (3–6). More than 90% of all bladder cancers are TCC, 5%–10% are squamous cell carcinoma (SCC), and the remaining 2%–3% are adenocarcinoma (3,6–10). SCC is associated with chronic inflammation, whereas adenocarcinoma is associated with persistent urachal remnants (3,11). Bladder cancers are commonly located in the trigone and its adjacency (4–10). The second most common location of TCC is the renal pelvis (1,11). It has a tendency to be multifocal and of low grade, similar to in the bladder (1,3). TCC of the urethra commonly involves the distal portion and tends to be superficial, but it behaves more aggressively, unlike in the bladder (4–8). Other rare urinary system tumors are lipoma, fibroma, leiomyoma, hemangioma, sarcoma, lymphoma, mesodermal tumors, carcinoid tumors, and pheochromocytoma, and these should be considered in differential diagnosis (12).

Etiology

Risk factors for TCC include smoking, analgesics (i.e. phenacetin), carcinogens (arsenic), schistosomiasis, familial cancer syndromes, and renal papillary necrosis (4). Smoking increases the risk 4-fold (13). Balkan nephropathy, which is seen in Europe, also increases the risk for TCC (14). TCC tends to be multifocal and highly recurrent (5,15).

Staging

Pathologic staging

Urothelial tumors are grouped into 2 types, based on their morphology, as invasive and superficial. Superficial ones are usually papillary, of low grade,

Received: 13.11.2011 – Accepted: 11.04.2012
Department of Radiology, Atatürk Training and Research Hospital, Bilkent, Ankara – TURKEY
Correspondence: *Oktay ALĞIN, Department of Radiology, Atatürk Training and Research Hospital, Bilkent, Ankara – TURKEY*
E-mail: droktayalgin@gmail.com

and limited to the mucosa lamina propria (3). They rarely metastasize; however, recurrence after treatment is common with a good prognosis (5,16). Invasive ones, however, generally appear smooth and develop from high-grade in situ lesions; they are localized to the surface epithelium. They appear as hyperemic mucosa at cystoscopy (3). Carcinoma in situ lesions can manifest with tumor cells in urine cytology and are known as precursors of invasive cancers (17).

Renal pelvis tumors are generally malignant; they involve both kidneys equally and are more commonly seen in males (8). Well-differentiated tumors are Grade I and intermediately differentiated ones are Grade II, whereas poorly differentiated tumors are Grade III (16).

Clinical staging

Clinical staging is done according to tumor–node–metastasis (TNM) classification (3). An analysis of the depth and spread of the tumor and lymph node involvement and a metastases workup are performed (2). Locally, they may involve the bladder orifice and trigone, ureters, uterus, vagina, urethra, vagina, prostate, and rectum (3–8,11). Lymphatic spread occurs through the paravesical, obturator, external iliac, and paraaortic lymph nodes, whereas hematogenous spread includes the liver, lungs, bones, and adrenal glands (2–5,18). Common iliac and paraaortic lymph node involvements are also considered as distant metastases (1).

Tumor staging (2,3)

Tx: Absence of an evaluable primary tumor.

T0: No tumor.

Tis: Carcinoma in situ.

Ta: Papillary tumor in the epithelium (Figure 1a).

T1: Lamina propria is invaded by the tumor.

T2: Muscular layer is invaded by the tumor (Figure 1b).

T2a: Superficial muscular layer is invaded by the tumor.

T2b: Deep muscular layer invaded by the tumor.

T3: Perivesical fat planes are invaded.

T3a: Microscopic invasion of the perivesical fat planes.

T3b: Macroscopic invasion of the perivesical fat planes.

T4a: Adjacent organs (prostate, rectum, and vagina) are invaded by the tumor (Figure 2).

T4b: Abdomen–pelvic wall is invaded by the tumor.

Lymph nodes

Nx: Nodal metastases are unknown.

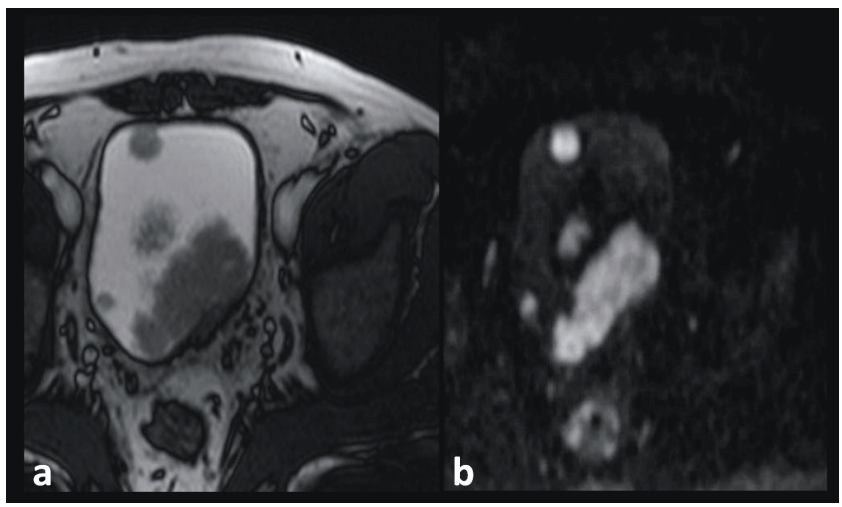

Figure 1. A patient with papillary bladder cancer (TNM staging: T2b): a) axial T2-weighting MR image demonstrates multiple, projectile, papillary masses in the bladder, and b) axial diffusion-weighted image also localizes these masses with a hyperintense signal pattern.

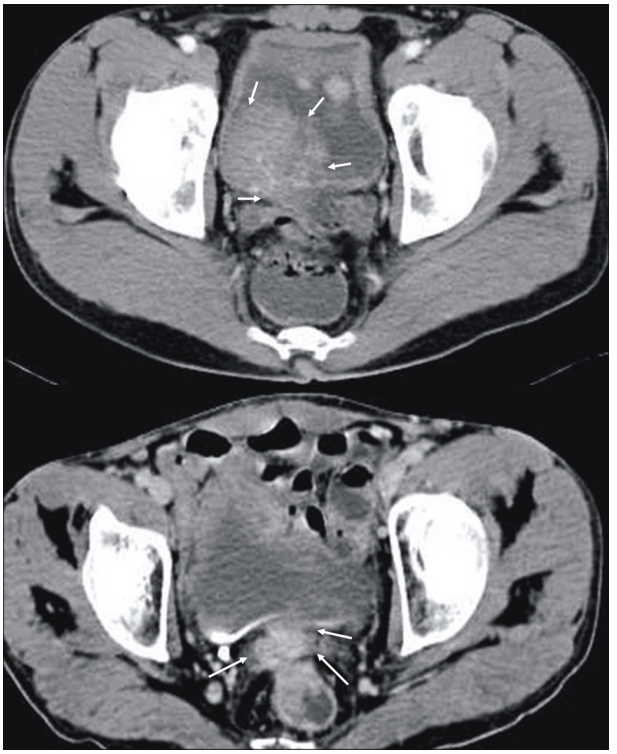

Figure 2. Axial CT images of a bladder cancer patient (T4 disease with seminal vesicle invasion) shows multiple focal wall thickening and a right posterolaterally localized mass (arrows) extruding from the wall into the lumen with contrast material enhancement (arrows) (upper image). The perivesical fat planes and perirectal space are both invaded by the lesion (arrows) (lower image).

Figure 3. Axial CT images of a bladder cancer patient show a right bladder wall mass (star) (upper image) with enhancing perivesical and perirectal lymph nodes (arrows), which correspond to N2 disease (lower image).

N1: Single pelvic lymph node less than 2 cm in diameter (Figure 3a).

N2: Pelvic lymph node metastases with a diameter of 2 cm to 5 cm (Figure 3b).

N3: Pelvic lymph node metastases greater than 5 cm in diameter.

Metastases

MX: Distant metastases are unknown.

M0: Absence of distant metastases.

M1: Presence of distant metastases.

Imaging techniques for diagnosis

Conventional cystoscopy is the gold standard of diagnostic methods (1–3). Imaging methods for diagnosis include intravenous pyelography (IVP), ultrasound (US), computed tomography (CT), and magnetic resonance imaging (MRI). The role of the direct urinary system radiograph is limited to depicting the presence of calcification and gas in the collecting system (2). IVP is less sensitive in the detection of smaller lesions (10). US is usually used as a first-line method and is sensitive in the detection of bladder tumors. US can be performed by transabdominal, transrectal, or transurethral approaches. CT is the most commonly used method for evaluation of the primary tumor, lymph nodes, and metastases (1). MRI is more sensitive than CT due to its superior soft tissue contrast resolution and it is useful in the investigation of tumoral depth penetration, distant metastases, bony involvement, and late fibrosis versus recurrence distinction (19–22).

Intravenous pyelography

IVP is the traditional initial imaging method in the imaging workup of hematuria (2). At the initial step of IVP, a direct urinary system radiograph should be

obtained prior to the contrast injection in order to visualize any opacity (10). IVP has nephrography, pyelography, and cystography phases (2). Large tumors appear as filling defects at the pyelography and cystography phases (23), whereas small tumors and intradiverticular lesions may not be visualized via this imaging method (10). The main limitation of this method is the radiation exposure. Additionally, as it includes an intravenous iodine-based contrast agent, it is contraindicated in patients with kidney failure and contrast allergy history (2,21,23). IVP has an accuracy range of 26% to 87% in the detection of bladder cancers with a smallest detected lesion size cutoff of 1.5 cm (2,9,10,23).

Ultrasound

US is a relatively cheaper and more accessible imaging method and is used as a first-line technique for the imaging workup of hematuria. US can precisely depict bladder and pelvis tumors in experienced hands but is limited in ureteral lesions due to gas superposition (2). Hydronephrosis of the kidneys, stones, cysts, and other filling defects within kidney collecting systems can be easily demonstrated at US, whereas bladder lesions appear as a projectile mass or wall thickening (2) (Figure 4). The disruption of the echogenic line around the bladder wall at US represents a possible invasion in bladder cancer patients (23).

A relatively less invasive nature, lack of any requirement for an intravenous contrast agent, and repeatability are among the main advantages of US; however, operator dependence, difficulty in cases of patient obesity, and abdominal gas superposition are among the main disadvantages of this technique. Bladder lesions that are smaller than 5 mm and localized to the bladder dome or neck can be missed via US (2,23). The overall accuracy of US for bladder cancer detection is around 82%–95% regardless of the lesion size (24,25). US can be limited in visualization of the distal renal pelvis, where IVP and CT have more success, but hydronephrosis secondary to tumors can be detected and graded by US (9,10). Additionally, US can be helpful in the evaluation of patients with sepsis, when IVP is contraindicated. Finally, Kocakoc et al. recently reported that virtual (3-dimensional) ultrasonographic cystoscopy can be a useful alternative for the evaluation of bladder cancers (26).

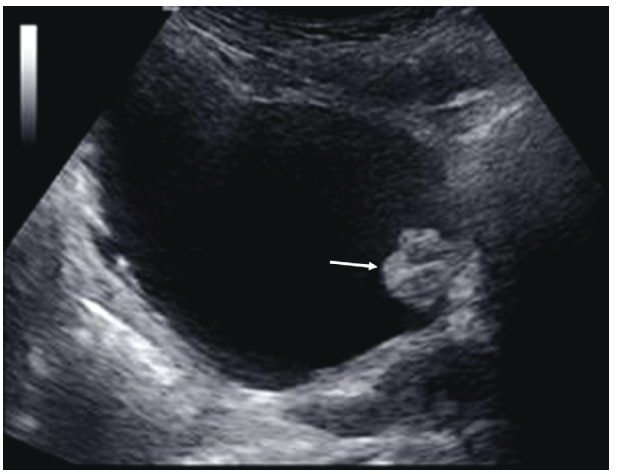

Figure 4. Axial ultrasound image of a patient with papillary carcinoma shows a projectile mass in the left bladder wall (arrow).

Computed tomography

CT is the most commonly used imaging method for urinary system tumors, especially in staging (9,10). The advent of multidetector technology has increased its use and utility in the evaluation of urinary system tumors. A standard abdomen CT scan includes an intravenous injection of 100–120 mL of nonionic contrast material, at an injection rate of 2.5–3 mL/s and a subsequent image acquisition at the parenchymal phase, with an approximate delay of 60–100 s following the injection (2,27). Kidney parenchyma and tumor enhancement can be evaluated at the nephrographic phase (9,10) (Figure 5). Epithelial tumors can be assessed more accurately at the excretory or pyelographic phase and they appear as filling defects (1,2) (Figure 6). The bladder should be sufficiently full and distended for proper lesion evaluation (Figure 7). Reconstructed images in various planes enable better evaluation of lesions localized to the dome and base of the bladder (27) (Figure 7). In some patients, ureteral lesions can be barely visualized, especially if there is incomplete opacification (9,10). In addition to routine CT scans, several special methods can also be used. These are summarized below.

CT urography

CT urography is the cross-sectional analog of IVP. In this technique, image acquisition is performed at 7–15 min after the intravenous contrast injection and

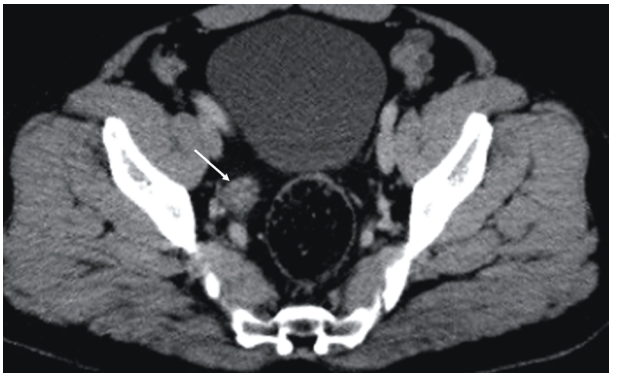

Figure 5. Axial CT image of a patient with ureteral carcinoma shows a nodular wall thickening of the distal right ureter with heterogeneous contrast enhancement and luminal narrowing (arrow).

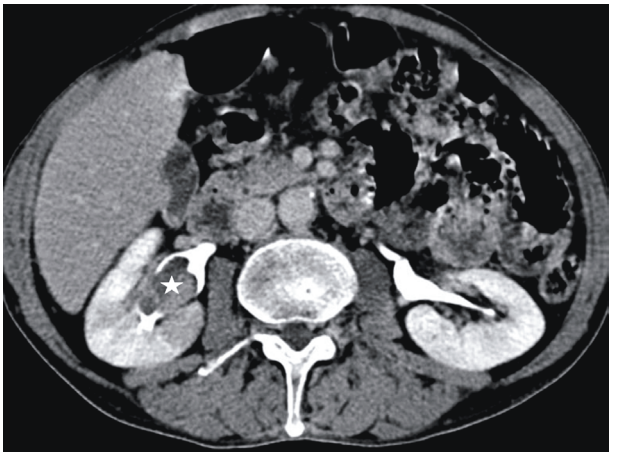

Figure 6. Axial CT image at the pyelography phase shows a hypodense filling defect in the right renal pelvis, which is consistent with a TCC (star).

the images are usually evaluated after a maximum intensity projection (MIP) reconstruction algorithm application (9,10). Tumors appear as focal wall thickening or as masses projecting into the lumen (9,10). The usage of multidetector scanners increases both the sensitivity of this technique as well as enables a more accurate depiction of lesions smaller than 4 mm (28).

Antegrade CT pyelography

In this technique, the renal pelvis is imaged following catheterization after a subsequent contrast injection through the catheter. In patients with kidney failure, this technique allows for the determination of the obstruction site without an intravenous contrast injection (2). Moreover, this technique can be considered as an alternative in patients with contrast allergy (Figure 8) (29). However, the invasiveness of this technique is a major drawback.

CT cystoscopy and virtual cystoscopy

This technique enables images to be obtained that are similar to those of conventional cystoscopy. However, its major limitations are the lack of real-time tissue sampling (biopsy), the inability to evaluate mucosa and carcinoma in situ, and the less accurate demonstration of very small lesions (23,30,31). On the other hand, it has some advantages over conventional cystoscopy, such as the fact that it can be easily performed as a noninvasive alternative in patients with benign prostate hyperplasia, bladder infections, urethral strictures, and prostatitis, when the conventional technique is contraindicated (32). Additionally, virtual cystoscopy is more successful in the evaluation of the bladder neck and in diverticula with a narrow neck, where the conventional technique is limited (32,33). The virtual cystoscopy method allows for a 360° visualization of the bladder on all planes, similar to or even better than the conventional method (32). Through this technique, the location and texture of the lesion can be assessed prior to biopsy or surgery, and this can aid in surgical planning and reduce the procedure time. Moreover, it can be used at the follow-up, as well (30–33) (Figure 9).

In this technique, the bladder is filled directly with air (minimally invasive, through a Foley catheter) or indirectly with intravenous contrast material (noninvasively). The air-filled approach requires 2 CT data sets (prone and supine) and therefore has a higher radiation dose exposure. The indirect method is performed at a supine position with a lower radiation dose exposure (34). However, in the indirect approach, virtual images can be obscured by artifacts secondary to the improper mixture of the contrast material and urine, especially in the increased trabeculation areas of the bladder wall (35).

Magnetic resonance imaging

MR urography

MR urography (MRU) can be used for patients with an iodine-based contrast material allergy or minimal renal insufficiency instead of CT urography

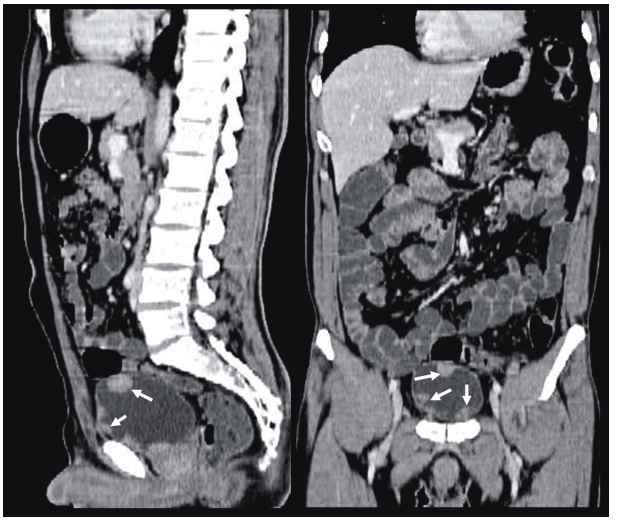

Figure 7. Sagittal (left) and coronal (right) reconstructed CT images show multiple, projectile enhancing tumor lesions in the bladder (arrows).

(20,21,36). Under such circumstances, it is safer to use macrocyclic MRI contrast agents (21). MRU has both static and functional components. In the static part (also called a noncontrast-enhanced or static MRU), heavily T2-weighted sequences are obtained without a contrast material injection, whereas in the functional part (also called a contrast material-enhanced or excretory MRU), the contrast-enhanced 3D gradient echo (GRE) T1-weighted sequences are acquired (20,37–39). Noncontrast-enhanced MRU (NCE-MRU) has less sensitivity for the detection of smaller lesions (37).

In contrast-enhanced MRU (CE-MRU), intravenous furosemide (10–20 mg) can be used to avoid the T2* effect of the contrast dilution and to distend the urinary system sufficiently (40). The most important postcontrast T1-weighted images are those obtained at the nephrographic and pyelographic phases. Smaller lesions appear as enhancing foci at the nephrographic phase, whereas they appear as a filling defect at the delayed excretory phase (36). Ureteral lesions can be visualized in either of these sequences (10).

Papillary tumors are seen as filling defects at MRU (36). Postcontrast T1-weighted images at the nephrographic phase are helpful for diagnosis and such lesions can be differentiated from others by their uniform homogeneous contrast enhancement

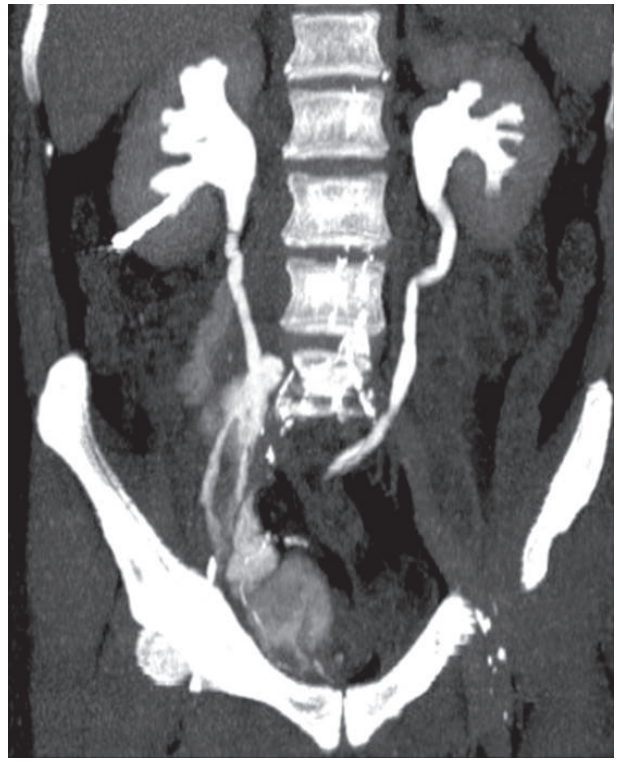

Figure 8. MIP image of an antegrade CT pyelogram of S/P surgery bladder cancer patient obtained following contrast injection through bilateral nephrostomy catheters.

(41). Flat lesions are challenging to depict due to hyperintense urine on T2-weighted sequences or at NCE-MRU and can be easily missed. CE-MRU is more useful in the diagnosis of such lesions (10,40,41).

MR cystography and virtual MR cystoscopy

About 80% of bladder cancers are polypoid, and MR cystography and virtual MR cystoscopy are important in localizing such lesions (41). On T2-weighted images, since urine appears hyperintense, it is easier to visualize pathologies with different signal characteristics. Virtual cystoscopy is obtained through the postprocessing of the T2-weighted data with multiplanar reconstruction and MIP algorithms. MR cystoscopy has higher sensitivity and specificity for lesions greater than 10 mm, whereas these values diminish for lesions smaller than 10 mm. Virtual cystoscopy performed with multidetector CT has a better spatial resolution than that of MRI, and therefore it is more sensitive to smaller lesions. Mural

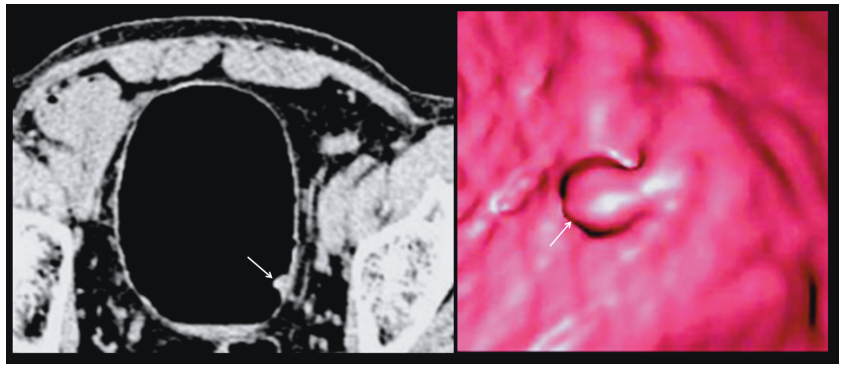

Figure 9. CT cystography (left) and virtual cystoscopy (right) images demonstrate a polypoid projectile lesion in the left lateral bladder wall (arrows). These figures reprinted permission from reference 31.

lesions and perivesical infiltration cannot be precisely detected at MR cystography. Moreover, in situ lesions cannot be identified, as there is no information about mucosal color changes (42,43).

The main advantages in using this technique as an alternative in case of a contraindication for the conventional cystoscopy are better localization of the bladder neck and intradiverticular lesions and the easiness of the follow-up of patients with local excision (44). The main disadvantages are operator dependency, inability to obtain real-time biopsy, higher cost, and the requirement of higher-strength magnet systems (42). The common indications for MR cystoscopy can be summarized as the need for bladder evaluation in case of urethral strictures, the investigation of bladder diverticula, and conditions in which conventional cystoscopy is contraindicated (42).

Diffusion-weighted MRI

Diffusion refers to the motion of the water molecules in biologic tissues following excitation via heat, which is also known as Brownian motion (45–47). Cancers appear as hyperintense foci on diffusion-weighted MRI (DW MRI) whereas they are hypointense on apparent diffusion coefficient (ADC) maps derived from DW MRI, and this may help to distinguish low-grade lesions from high-grade ones (48). ADC is a reliable quantitative measure and ADC values can help to differentiate cancers from cystitis or wall hypertrophy secondary to outlet obstruction (45–47).

Differential diagnosis

Filling defects, which are among the most common imaging features of urothelial tumors, can also be seen in other pathologies that also result in diffuse enhancement, wall thickening, and focal infiltration

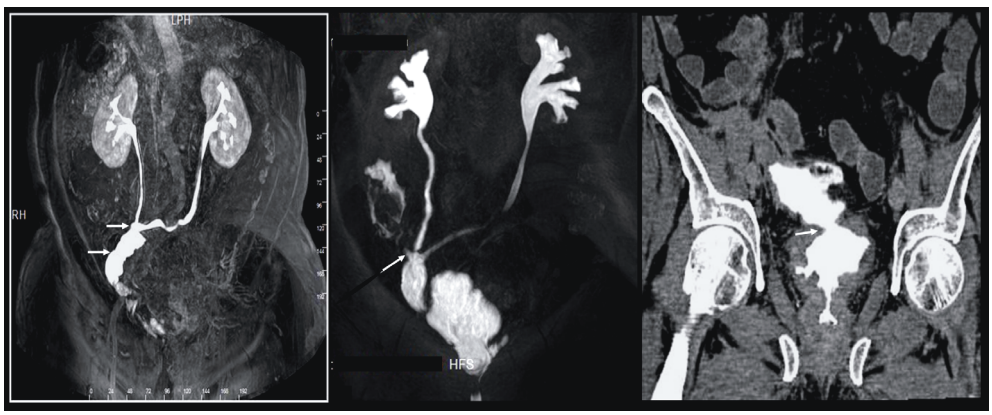

Figure 10. CE-MRU and multidetector CT images of 3 different patients. Coronal postcontrast 3D T1-weighting gradient-echo MR image (CE-MRU) in a patient with ileal conduit shows a patent passage (arrows in left image). Coronal CE-MRU image of a different patient shows a leak from the anastomoses (arrow in middle image). Right image shows bladder perforation at the postoperative stage.

(10). Stone, clot, mucous, debris, fungus ball, concentrated gadolinium, flow-related artifacts, vascular partial volume, inflammation, reflux, peristaltic motion, and jet flow should be considered in the differential diagnosis of urothelial carcinoma (35–37,49–51). Additionally, nephrostomy tubes, instrumentations, urinary stasis, intravesical chemotherapy agents, neobladder and urinary diversions, and urinary stents can mimic diffuse contrast enhancement, as well (1,2).

Lymph node metastasis

Spherical lymph nodes greater than 8 mm, oval or ellipsoid nodes greater than 10 mm with rapid enhancement at dynamic scans, and clustered lymph nodes are important findings for metastatic involvement (1–4,52). A few publications have reported that ADC values can be helpful in differentiating benign nodes from malignant ones; however, further research is required to explore this topic (53).

Surgical treatment of bladder tumors

Treatment approach varies with patient age and comorbidities. The aim of the treatment in superficial (stage T1) lesions is to prevent recurrence or progression. A bladder-sparing treatment is applied in early-stage tumors, and partial cystectomy or transurethral tumor resections are among such techniques (54). In situ lesions tend to be high grade and they may require cystectomy if there is no response to 2 episodes of bacillus Calmette-Guérin treatment for 6 weeks. T2 and T3 lesions usually require cystectomy as they have infiltrative characteristics in the presence of nodal infiltration, and chemotherapy and radiotherapy should be added to the treatment regimen. Cystectomy is a well-known standard treatment for patients with invasive tumor (54,55). After pelvic surgery, bleeding is a common and significant risk. Techniques of interventional radiology are noninvasive and safe methods for demonstration of the bleeding area and effective treatment (56).

An artificial bladder is reconstructed in cystectomy and this is known as a diversion procedure. Several diversion techniques exist:

Urinary diversions

They are mainly grouped into 2 types.

Noncontinent diversions (ureterostomy and conduits): In ureterostomy, ureters are directly attached to the skin without an intestinal loop. This includes 2 stomas and a pouch. This technique is rarely used. In case of an ileal conduit, a reservoir is created from a short segment of the small bowel and the ureters are attached to one side of this loop, whereas the other side is attached to the skin to make up the stoma (Figure 10). An additional pouch is also created in the opening of the stoma. This technique is well established with long-term complication and collecting system dilatation rates of 30% and 20%, respectively (57).

Continent diversions: These are grouped into 2 types: heterotopic and orthotopic. Heterotopic diversion operations are not performed commonly nowadays. The most common of them includes stomatization of the ureters to the sigmoid colon, but this increases the infection rate. Orthotopic diversions are more commonly preferred recently and a new bladder is formed using a small bowel loop, which replaces the excised bladder. Ureters are connected to this newly formed bladder and the patient can perform urinary excretion properly (58) (Figure 10). Complications such as perforation, fistula formation, bleeding, and urinoma can be seen at the postoperative phase (54–58) (Figure 10).

Conclusion

Urothelial cancers usually present with painless hematuria and are currently more commonly diagnosed secondary to recent developments in the imaging technology. The application of an accurate imaging algorithm to further investigate painless hematuria will enable prompt and correct diagnosis of urothelial cancers, which will increase the yield of treatment and significantly decrease cancer and treatment-related morbidity and mortality. Moreover, the angiographic techniques can be useful in the pre- and postoperative period management of patients with urothelial cancer.

Acknowledgments

The authors thank Dr Barış Türkbey, Dr Gökçe Akgündüz, and Dr E. Bengi Türkbey for their contributions.

References

1. Lee EK, Dickstein RJ, Kamta AM. Imaging of urothelial cancers: what the urologist needs to know. AJR Am J Roentgenol 2011; 196: 1249–54.
2. Gödekmerdan A, Yahşi S, Semerciöz A, İlhan F, Akpolat N, Yekeler H. Determination of nuclear matrix protein 22 levels in cystitis, urothelial dysplasia and urothelial carcinoma. Turk J Med Sci 2006; 36: 93–6.
3. Wong-You-Cheong JJ, Woodward PJ, Manning MA, Sesterhenn IA. From the archives of the AFIP: neoplasms of the urinary bladder: radiologic-pathologic correlation. Radiographics 2006; 26: 553–80.
4. Ng CS. Radiologic diagnosis and staging of renal and bladder cancer. Semin Roentgenol 2006; 41: 121–38.
5. Vikram R, Sandler CM, Ng CS. Imaging and staging of transitional cell carcinoma. Part 1. Lower urinary tract. AJR Am J Roentgenol 2009; 192: 1481–7.
6. Vikram R, Sandler CM, Ng CS. Imaging and staging of transitional cell carcinoma. Part 2. Upper urinary tract. AJR Am J Roentgenol 2009; 192: 1488–93.
7. Browne RF, Meehan CP, Colville J, Power R, Torreggiani WC. Transitional cell carcinoma of the upper urinary tract: spectrum of imaging findings. Radiographics 2005; 25: 1609–27.
8. Lakadamyalı H, Akata D, Akdoğan B, Akhan O. Multicentric uroepithelial tumor: CT and MRI findings. Diagn Intervent Radiol 2002; 8: 85–9.
9. Caoili EM, Cohan RH, Inampudi P, Ellis JH, Shah RB, Faerber GJ et al. MDCT urography of upper tract urothelial neoplasms. AJR Am J Roentgenol 2005; 184: 1873–81.
10. Akbulut Z, Tuzlalı M, Canda AE, Ercan K, Kandemir O, Balbay MD. Factors affecting adrenal gland involvement in patients who underwent radical nephrectomy for renal cell carcinoma. Turk J Med Sci 2009; 39: 215–22.
11. Rafla S. Tumors of the upper urothelium. Am J Roentgenol Radium Ther Nucl Med 1975; 123: 540–51.
12. Mostofi FK: Histological typing of urinary bladder tumours. Berlin: Springer-Verlag; 1999. p.3–27.
13. Bostwick DG, Ramnani D, Cheng L. Diagnosis and grading of bladder cancer and associated lesions. Urol Clin North Am 1999; 26: 493–507.
14. Stefanovic V, Radovanovic Z. Balkan endemic nephropathy and associated urothelial cancer. Nat Clin Pract Urol 2008; 5: 105–12.
15. Elmajian DA. Transitional cell carcinoma of the ureter and renal pelvis. In: Nachtsheim D, editor. Urological oncology. Austin (TX): Landes Bioscience; 2005. p.43–52.
16. Fleshner N, Kondylis F. Demographics and epidemiology of urothelial cancer of urinary bladder. In: Droller MJ, editor. Urothelial tumors. Hamilton (ON): Decker; 2004. p.1–16.
17. Pashos CL, Botteman MF, Laskin BL, Redaelli A. Bladder cancer: epidemiology, diagnosis, and management. Cancer Pract 2002; 10: 311–22.
18. Greene FL, Compton CC, Fritz AG, Shah JP, Winchester DP. AJCC cancer staging atlas. Berlin, Germany: Springer-Verlag; 2006.
19. Cowan NC, Crew JP. Imaging bladder cancer. Curr Opin Urol 2010; 20: 409–13.
20. Algin O. Functional evaluation of kidneys: which technique is more useful? AJR Am J Roentgenol 2010; 194: W241.
21. Algin O. A new contrast media for functional MR urography: Gd-MAG3. Med Hypotheses 2011; 77: 74–6.
22. Türkbey B, Bernardo M, Merino MJ, Wood BJ, Pinto PA, Choyke PL. MRI of localized prostate cancer: coming of age in the PSA era. Diagn Interv Radiol 2012; 18: 34–45.
23. Rafique M, Javed AA. Role of intravenous urography and transabdominal ultrasonography in the diagnosis of bladder carcinoma. Int Braz J Urol 2004; 30: 185–91.
24. Malone PR, Weston-Underwood J, Aron PM, Wilkinson KW, Joseph AE, Riddle PR. The use of transabdominal ultrasound in the detection of early bladder tumours. Br J Urol 1986; 58: 520–2.
25. Itzchak Y, Singer D, Fischelovitch Y. Ultrasonographic assessment of bladder tumors. I. Tumor detection. J Urol 1981; 126: 31–3.
26. Kocakoc E, Kiris A, Orhan I, Poyraz AK, Artas H, Firdolas F. Detection of bladder tumors with 3-dimensional sonography and virtual sonographic cystoscopy. J Ultrasound Med 2008; 27: 45–53.
27. Ozbülbül NI, Dağli M, Akdoğan G, Olçer T. CT urography of a vesicourachal diverticulum containing calculi. Diagn Interv Radiol 2010; 16: 56–8.
28. Wang LJ, Wong YC, Ng KF, Chuang CK, Lee SY, Wan YL. Tumor characteristics of urothelial carcinoma on multidetector computerized tomography urography. J Urol 2010; 183: 2154–60.
29. Ghersin E, Brook OR, Meretik S, Kaftori JK, Ofer A, Amendola MA et al. Antegrade MDCT pyelography for the evaluation of patients with obstructed urinary tract. AJR Am J Roentgenol 2004; 183: 1691–6.
30. Song JH, Francis IR, Platt JF, Cohan RH, Mohsin J, Kielb SJ et al. Bladder tumor detection at virtual cystoscopy. Radiology 2001; 218: 95–100.
31. Arslan H, Ceylan K, Harman M, Yilmaz Y, Temizoz O, Can S. Virtual computed tomography cystoscopy in bladder pathologies. Int Braz J Urol 2006; 32: 147–54.
32. Tsampoulas C, Tsili AC, Giannakis D, Alamanos Y, Sofikitis N, Efremidis SC. 16-MDCT cystoscopy in the evaluation of neoplasms of the urinary bladder. AJR Am J Roentgenol 2008; 190: 729–35.
33. Frank R, Stenzl A, Frede T, Eder R, Recheis W, Knapp R et al. Three-dimensional computed tomography of the reconstructed lower urinary tract: technique and findings. Eur Radiol 1998; 8: 657–63.

34. Kim JK, Park SY, Kim HS, Kim SH, Cho KS. Comparison of virtual cystoscopy, multiplanar reformation, and source CT images with contrast material-filled bladder for detecting lesions. AJR Am J Roentgenol 2005; 185: 689–96.

35. Nambirajan T, Sohaib SA, Muller-Pollard C, Reznek R, Chinegwundoh FI. Virtual cystoscopy from computed tomography: a pilot study. BJU Int 2004; 94: 828–31.

36. Takahashi N, Kawashima A, Glockner JF, Hartman RP, Kim B, King BF. MR urography for suspected upper tract urothelial carcinoma. Eur Radiol 2009; 19: 912–23.

37. Takahashi N, Kawashima A, Glockner JF, Hartman RP, Leibovich BC, Brau AC et al. Small (<2-cm) upper-tract urothelial carcinoma: evaluation with gadolinium-enhanced three-dimensional spoiled gradient-recalled echo MR urography. Radiology 2008; 247: 451–7.

38. Broome DR, Girguis MS, Baron PW, Cottrell AC, Kjellin I, Kirk GA. Gadodiamide-associated nephrogenic systemic fibrosis: why radiologists should be concerned. AJR Am J Roentgenol 2007; 188: 586–92.

39. Morcos SK. Extracellular gadolinium contrast agents: differences instability. Eur J Radiol 2008; 66: 175–9.

40. Nolte-Ernsting CC, Bücker A, Adam GB, Neuerburg JM, Jung P, Hunter DW et al. Gadolinium-enhanced excretory MR urography after low-dose diuretic injection: comparison with conventional excretory urography. Radiology 1998; 209: 147–57.

41. Merkle EM, Wunderlich A, Aschoff AJ, Rilinger N, Görich J, Bachor R et al. Virtual cystoscopy based on helical CT scan datasets: perspectives and limitations. Br J Radiol 1998; 71: 262–7.

42. Beer A, Saar B, Zantl N, Link TM, Roggel R, Hwang SL et al. MR cystography for bladder tumor detection. Eur Radiol 2004; 14: 2311–9.

43. Fenlon HM, Bell TV, Ahari HK, Hussain S. Virtual cystoscopy: early clinical experience. Radiology 1997; 205: 272–5.

44. Läemmle M, Beer A, Settles M, Hannig C, Schwaibold H, Drews C. Reliability of MR imaging based virtual cystoscopy in the diagnosis of cancer of the urinary bladder. AJR Am J Roentgenol 2002; 178: 1483–8.

45. Matsuki M, Inada Y, Tatsugami F, Tanikake M, Narabayashi I, Katsuoka Y. Diffusion-weighted MR imaging for urinary bladder carcinoma: initial results. Eur Radiol 2007; 17: 201–4.

46. Takahara T, Imai Y, Yamashita T, Yasuda S, Nasu S, Van Cauteren M. Diffusion weighted whole body imaging with background body signal suppression (DWIBS): technical improvement using free breathing, STIR and high resolution 3D display. Radiat Med 2004; 22: 275–82.

47. Shimofusa R, Fujimoto H, Akamata H, Motoori K, Yamamoto S, Ueda T et al. Diffusion-weighted imaging of prostate cancer. J Comput Assist Tomogr 2004; 29: 149–53.

48. Türkbey B, Aras Ö, Karabulut N, Turgut AT, Akpınar E, Alibek S et al. Diffusion-weighted MRI for detecting and monitoring cancer: a review of current applications in body imaging. Diagn Interv Radiol 2012; 18: 46–59.

49. Blandino A, Gaeta M, Minutoli F, Salamone I, Magno C, Scribano E et al. MR urography of the ureter. AJR Am J Roentgenol 2002; 179: 1307–14.

50. Heneghan JP, Dalrymple NC, Verga M, Rosenfield AT, Smith RC. Soft-tissue "rim" sign in the diagnosis of ureteral calculi with use of unenhanced helical CT. Radiology 1997; 202: 709–11.

51. Chahal R, Taylor K, Eardley I, Lloyd SN, Spencer JA. Patients at high risk for upper tract urothelial cancer: evaluation of hydronephrosis using high resolution magnetic resonance urography. J Urol 2005; 174: 478–82.

52. Jager GJ, Barentsz JO, Oosterhof GO, Witjes JA, Ruijs SJ. Pelvic adenopathy in prostatic and urinary bladder carcinoma: MR imaging with a three-dimensional TI-weighted magnetization-prepared-rapid gradient-echo sequence. AJR Am J Roentgenol 1996; 167: 1503–7.

53. Chen YB, Liao J, Xie R, Chen GL, Chen G. Discrimination of metastatic from hyperplastic pelvic lymph nodes in patients with cervical cancer by diffusion-weighted magnetic resonance imaging. Abdom Imaging 2011; 36: 102–9.

54. Oosterlinck W, Lobel B, Jakse G, Malmström PU, Stöckle M, Sternberg C et al. Guidelines on bladder cancer. Eur Urol 2002; 41: 105–12.

55. Cookson MS, Herr HW, Zhang ZF, Soloway S, Sogani PC, Fair WR. The treated natural history of high risk superficial bladder cancer: 15-year outcome. J Urol 1997; 158: 62–7.

56. Karaman B, Oren NC, Andic C, Ustunsoz B. Transcatheter embolization for the treatment of both vaginal and lower intestinal bleeding due to advanced pelvic malignancy. Eurasian J Med 2010; 42: 153–6.

57. Neal DE. Complications of ileal conduit diversion in adults with cancer followed up for at least five years. Br Med J (Clin Res Ed) 1985; 290: 1695–7.

58. Hautmann RE, de Petriconi R, Gottfried HW, Kleinschmidt K, Mattes R, Paiss T. The ileal neobladder: complications and functional results in 363 patients after 11 years of follow up. J Urol 1999; 161: 422–7.